Thermal Destabilization of Rhodopsin and Opsin by Proteolytic Cleavage in Bovine Rod Outer Segment Disk Membranes†

Judith S. Landin, Madan Katragadda, and Arlene D. Albert*

Department of Molecular and Cell Biology, University of Connecticut, Storrs, Connecticut 06269

Received January 9, 2001; Revised Manuscript Received May 17, 2001

ABSTRACT: The G-protein coupled receptor, rhodopsin, consists of seven transmembrane helices which are buried in the lipid bilayer and are connected by loop domains extending out of the hydrophobic core. The thermal stability of rhodopsin and its bleached form, opsin, was investigated using differential scanning calorimetry (DSC). The thermal transitions were asymmetric, and the temperatures of the thermal transitions were scan rate dependent. This dependence exhibited characteristics of a two-state irreversible denaturation in which intermediate states rapidly proceed to the final irreversible state. These studies suggest that the denaturation of both rhodopsin and opsin is kinetically controlled. The denaturation of the intact protein was compared to three proteolytically cleaved forms of the protein. Trypsin removed nine residues of the carboxyl terminus, papain removed 28 residues of the carboxyl terminus and a portion of the third cytoplasmic loop, and chymotrypsin cleaved cytoplasmic loops 2 and 3. In each of these cases the fragments remained associated as a complex in the membrane. DSC studies were carried out on each of the fragmented proteins. In all of the samples the scan rate dependence of the T_m indicated that the transition was kinetically controlled. Trypsin-proteolyzed protein differed little from the intact protein. However, the activation energy for denaturation was decreased when cytoplasmic loop 3 was cleaved by papain or chymotrypsin. This was observed for both bleached and unbleached samples. In the presence of the chromophore, 11-*cis*-retinal, the noncovalent interactions among the proteolytic fragments produced by papain and chymotrypsin cleavage were sufficiently strong such that each of the complexes denatured as a unit. Upon bleaching, the papain fragments exhibited a single thermal transition. However, after bleaching, the chymotrypsin fragments exhibited two calorimetric transitions. These data suggest that the loops of rhodopsin exert a stabilizing effect on the protein.

The structures of integral membrane proteins must accommodate interactions with both the hydrocarbon core of the lipid bilayer in which they are imbedded and the aqueous phase into which they protrude. The stability of membrane proteins is thus influenced by two different environments as well as by intermolecular interactions. Though there are far fewer studies of the stability of membrane proteins than are available for soluble proteins, it appears that the protein regions which interact with the aqueous phase behave in a manner similar to that of soluble proteins while those within the hydrophobic core are more structurally stable (*1*, *2*). Cytochrome b_5 provided an early example of the domain nature of membrane proteins. The two circular dichroism transitions exhibited by this protein were interpreted to represent the aqueous and transmembrane domains (*3*). For membrane proteins that traverse the bilayer multiple times, the relative importance of the extramembranous regions and intramembraneous regions to overall protein stability poses an interesting problem. For example, it has been shown that some of the helices of bacteriorhodopsin will associate properly without covalently linked loop regions (*4*, *5*). However, while the contribution of each loop to protein stability is small, it has been predicted that loss of all loops would lead to instability of bacteriorhodopsin at room temperature (*4*).

The visual pigment, rhodopsin, is the most extensively studied member of the family of G-protein receptors. Since rhodopsin constitutes greater than 90% of the disk membrane protein (*6*, *7*), measurements made on the proteins of disk membranes predominantly reflect the properties of rhodopsin in its native environment. Rhodopsin consists of seven transmembrane helices connected by loop domains (*8*, *9*). Light sensitivity is conferred by the presence of 11-*cis*-retinal. Upon absorption of light, 11-*cis*-retinal undergoes a conformational change to *all*-*trans*-retinal. Regeneration of light sensitivity requires additional 11-*cis*-retinal.

Rhodopsin is stabilized by several structural features. These include the lipid bilayer, helix−helix interactions within the bilayer, the retinal chromophore, and the structures of the extramembranous regions. While data are available on the former issues, the extent to which the extramembranous portions of the protein contribute structural stability is unclear. Therefore, the contributions of the carboxyl terminus and cytoplasmic loops 2 and 3 to the thermal stability of rhodopsin were examined. These regions were selectively proteolyzed by trypsin, papain, and chymotrypsin (*10*), and the resulting protein fragments were subjected to thermal denaturation studies using differential scanning calorimetry

† This work is supported by National Institutes of Health Grant EY 03328.

* To whom correspondence should be addressed. Phone: (860) 486-5202. Fax: (860) 486-4331. E-mail: albert@uconnvm.uconn.edu.

10.1021/bi0100539 CCC: $20.00
Published on Web 08/24/2001

(DSC).[1] These studies suggest that denaturations of both the intact protein and the proteolytic fragments are kinetically modulated processes and that the loops play a role in the stabilization of the structure of rhodopsin to thermally induced denaturation.

EXPERIMENTAL PROCEDURES

Sample Preparation. Frozen bovine retinas were obtained from Lawson (Lincoln, NE). Osmotically intact disks were isolated from rod outer segments by Ficoll flotation according to Smith (*7*). All operations were carried out under dim red light. Rhodopsin concentration was determined from the change in absorbance at 500 nm upon bleaching in the presence of hydroxylamine.

Proteolysis was achieved by incubation of disk membranes with either trypsin, papain, or chymotrypsin at 37 °C for 3 h. In each of the samples, the rhodopsin concentration was approximately 1 mg/mL. TPCK-treated trypsin was added at a 1:10 ratio to disk membranes in 5 mM Tris/acetate, pH 7.4, and 0.14 mM $CaCl_2$. The reaction was stopped by addition of a 5-fold excess of soybean trypsin inhibitor. Papain proteolysis was carried in 100 mM phosphate, 2 mM EDTA, and 5 mM cysteine, pH 7.0, with a ratio of papain to rhodopsin of 1:20. The reaction was stopped by addition of iodoacetamide to a final concentration of 10 mM. TLCK-treated chymotrypsin was added at a 1:10 ratio in 10 mM Tris/acetate, pH 7.0. The reaction was stopped by addition of PMSF to a final concentration of 1 mM. Appropriate control samples were generated for each of the proteolyzed samples by incubating disks under identical conditions, but without the enzyme. These controls were subsequently found to behave identically and were pooled for all results. All samples were subsequently washed into in 10 mM potassium phosphate buffer, pH 7. Proteolysis was verified by a 10% SDS−PAGE (*11*). Gels were Coomassie stained and scanned on an Apple Color OneScanner 1200/30. Total protein concentration was determined by the method of Lowry (*12*).

Differential Scanning Calorimetry. Differential scanning calorimetry experiments were performed using a MicroCal VP-DSC microcalorimeter. Samples of 1−2 mg/mL of rhodopsin (opsin) in disks were run. For bleached samples, the protein was exposed to white light for 20 min in the presence of hydroxylamine. Each sample was scanned at 15°, 30°, 60°, and 90°/h. Each sample was scanned twice. Because the protein transitions are irreversible, the second scans were used to determine the baseline. Enthalpies were determined by curve fitting with the non-two-state algorithm MicroCal DSC version of the Origin software.

RESULTS

Differential Scanning Calorimetry Studies of Rhodopsin and Opsin. DSC experiments previously demonstrated that opsin denatures at a temperature approximately 15 °C lower than that of rhodopsin (*13*−*16*). In the present study excess heat capacity curves were obtained by differential scanning calorimetry for rhodopsin and opsin (Figure 1). In each case a single transition was observed. Consistent with previous observations for rhodopsin and for opsin, the DSC transitions are irreversible; upon rescanning the sample, no transition was observed. The calorimetric enthalpy of this transition was determined from the area under the curve and the transition temperature (T_m) from the midpoint of the peak.

Irreversible protein denaturation has been described by the Lumry−Eyring model (*17*). In this scheme, the native protein is in equilibrium with unfolded state(s). The unfolded state then undergoes an irreversible transition to the final denatured state:

$$N \leftrightarrow U \Rightarrow D$$

In this scheme the unfolded state is not limited to a single state, and although the term "unfolded" is used, considerable secondary structure may still be present. The consequences of this model have been investigated in detail elsewhere (*18*). Briefly, if the formation of D is slow relative to the rate of re-formation of N, the unfolded state will be highly populated while only a small amount of D will be present during the transition. In this case, the transition temperature will have little dependence on the scanning rate. However, if the rate of formation of D is rapid, a significant amount of D will be present during the transition and the transition temperature will exhibit a distinct dependence upon the scanning rate. In the former case, an equilibrium that exists just prior to the irreversible step dominates, and thermodynamic information can be obtained. However, the latter case can be approximated as a two-state irreversible process, and the kinetics of the formation of D determines the heat absorption. While the total enthalpy of the reaction can be obtained, other thermodynamic information cannot (*19*).

Kinetic information for a process approximated by the two-state irreversible model can be obtained by determining the dependence of the transition temperature on the scanning rate in the calorimeter (*19*−*21*). It has been shown for this model that the scanning rate and the transition temperature are related by the equation (*20*):

$$\ln(\text{scanning rate}/T_m^2) = \text{const} - E/RT_m$$

DSC measurements were made on rhodopsin and opsin at four scanning rates as described in Experimental Procedures. Asymmetric irreversible transitions were observed for both rhodopsin and opsin. The plot of $\ln(\text{scanning rate}/T_m^2)$ vs $1/T_m$ was linear (Figure 2). This behavior is consistent with a two-state irreversible denaturation process for the protein. The energy of activation (E) was determined from the slope of this line for both rhodopsin and opsin and is given in Table 1. The total enthalpy was determined calorimetrically and is also given in Table 1. The energy of this transition is less for opsin than for rhodopsin. The calorimetric enthalpy and the denaturation activation energy are essentially the same for the denaturation of rhodopsin and of opsin.

Differential Scanning Calorimetry of Proteolyzed Rhodopsin and Opsin. The role of the extramembranous loops and the carboxyl terminus in stabilizing both rhodopsin and opsin to thermal denaturation were investigated by determining the effect of proteolysis at specific extramembranous sites. Three enzymes were chosen to proteolyze different portions of the

[1] Abbreviations: DSC, differential scanning calorimetry; EDTA, ethylenediaminetetraacetic acid; PMSF, phenylmethanesulfonyl fluoride; SDS−PAGE, sodium dodecyl sulfate−polyacrylamide gel electrophoresis; TLCK, L-1-chloro-3-(4-tosylamido)-7-amino-2-heptanone; TPCK, L-1-tosylamido-2-phenylethyl chloromethyl ketone.

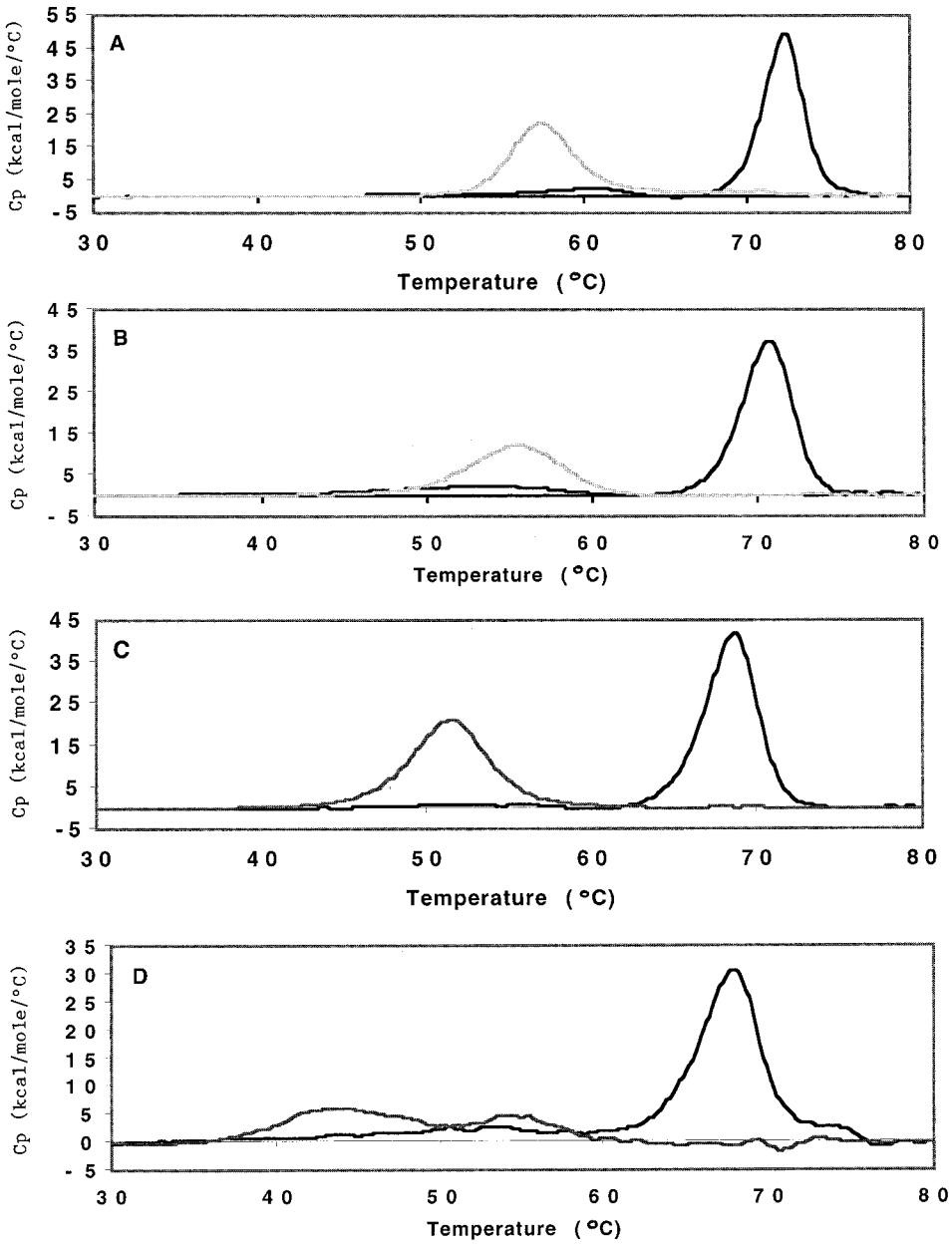

FIGURE 1: Examples of denaturation endotherms obtained by DSC at pH 7 with a scan rate of 1 deg/min: (A) rhodopsin (higher transition temperature) and opsin ((lower transition temperature), (B) trypsin-proteolyzed disk membranes, unbleached (higher transition temperature) and bleached (lower transition temperature), (C) papain-proteolyzed disk membranes unbleached (higher transition temperature) and bleached (lower transition temperature), and (D) chymotrypsin-proteolyzed disk membranes (higher transition temperature) and bleached (lower transition temperature).

cytoplasmic face of rhodopsin (Figure 3). Trypsin cleaves between residues 339 and 340, thus removing nine residues of the carboxyl terminus. Papain removes 27 residues of the carboxyl terminus and a portion of the third cytoplasmic loop between residues 236 and 241. Chymotrypsin cleaves cytoplasmic loops 2 and 3, at residues 146 and 244, respectively. Proteolysis was confirmed by SDS−PAGE and is shown in Figure 4. In agreement with previous studies (*22*, *23*), proteolysis of rhodopsin in the disk membrane by each of these enzymes did not cause a change in the absorption spectra. Therefore, studies of the protein could be carried out both on the unbleached protein and on the bleached protein.

Excess heat capacity curves were obtained by differential scanning calorimetry of the protolytic fragments both before and after bleaching (Figure 1). In each case, the DSC transitions were asymmetric and irreversible. Unbleached trypsin-, papain-, and chymotrypsin-proteolyzed rhodopsin exhibited a single transition. The total calorimetric enthalpies of these transitions were determined from the area under the curve and are presented in Table 1. The transition temperatures (T_m) were determined from the midpoint of the peaks and are presented in Table 2.

The scan rate dependence of the transition temperature was determined for the fragments produced by proteolysis. If the denaturation of the proteolytic fragments can be approximated by a two-state irreversible model, kinetic information can be obtained by determining the dependence of the transition temperature on the scanning rate as determined above for rhodopsin and opsin. DSC transitions

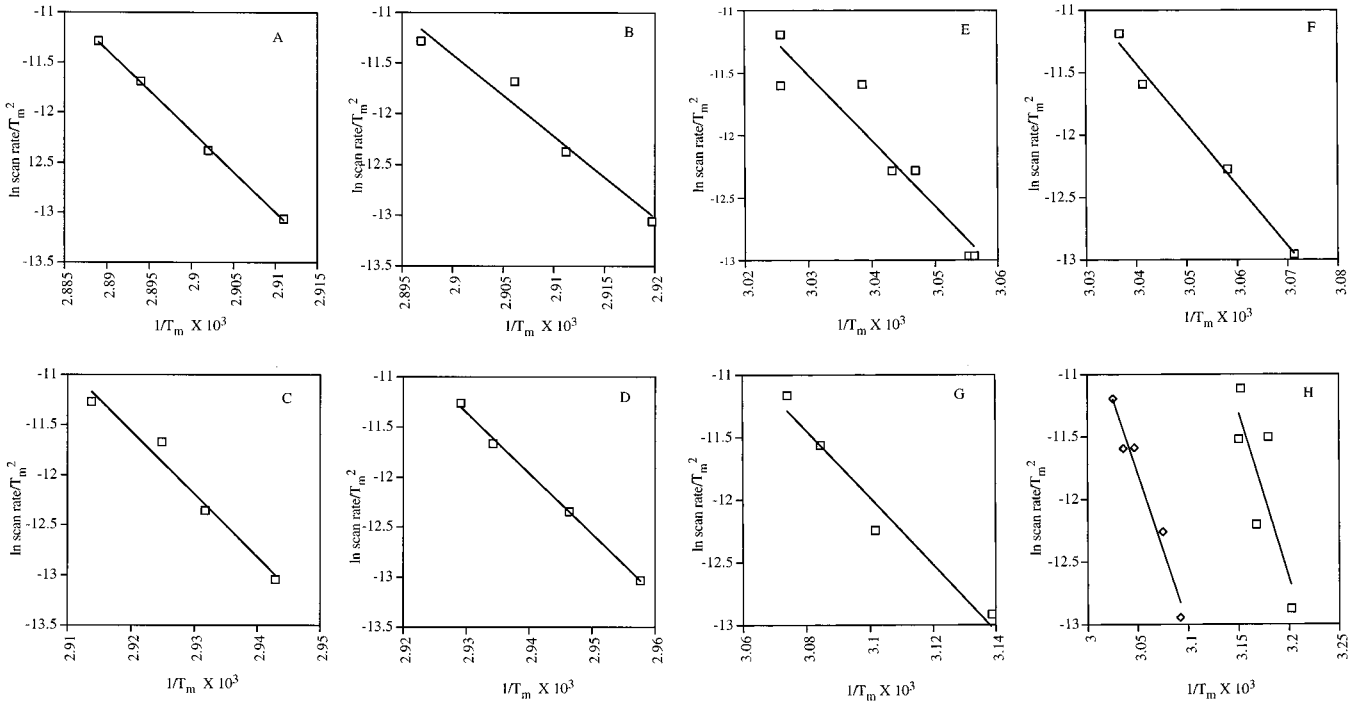

FIGURE 2: Plot of ln(scan rate/T_m^2) versus $1/T_m$ for proteolyzed disk membranes: (A) rhodopsin in disk membranes, (B) trypsin-proteolyzed disk membranes, unbleached, (C) papain-proteolyzed disk membranes, unbleached, (D) chymotrypsin-proteolyzed disk membranes, unbleached, (E) opsin in disk membranes, (F) trypsin-proteolyzed disk membranes, bleached, (G) papain-proteolyzed disk membranes, bleached, and (H) chymotrypsin-proteolyzed disk membranes, bleached. The scan rates used were 0.25, 0.5, 1.0, and 1.5 deg/min. Values for T_m are given in Table 2. Lines are best fit as determined by linear regression.

Table 1: Comparison of Enthalpy and Energy Values for Control and Proteolyzed Rhodopsin

		ΔH_{cal} (kcal/mol)	E (kcal/mol)
rhodopsin	unbleached	160	162
	bleached	101	100
trypsin	unbleached	119	160
fragment	bleached	81	98
papain	unbleached	148	126
fragment	bleached	115	53
chymotrypsin	unbleached	81	122
fragment	bleached (1)	43	61
	bleached (2)	29	48

[a] ΔH_{cal} determined by averaging ΔH_{cal} at each of the scan rates.

were obtained for each of the proteolytic fragments in both the unbleached and the bleached states at four scanning rates. For each case, the plot of ln(scanning rate/T_m^2) vs $1/T_m$ was linear (Figure 2). As was the case for rhodopsin and opsin, this behavior is consistent with a two-state irreversible denaturation process. The energies of activation (E) were determined from the slope of this line for both the unbleached and bleached forms and are given in Table 1. These activation energies and the total calorimetric enthalpies of the reaction were remarkably similar in almost all cases.

Upon bleaching, the trypsin- and papain-proteolyzed protein also exhibited a single transition. However, upon bleaching, the chymotrypsin fragment exhibited two distinct transitions. The trypsin fragment exhibited a DSC transition temperature only 1 deg lower than that observed for the intact protein for both the unbleached and bleached states at each of the scan rates. The denaturation activation energy was, within experimental error, unchanged from the intact protein in both the unbleached and bleached states. The papain fragments consist of helices 1, 2, 3, 4, and 5 and helices 6 and 7. These two fragments remain associated as a complex in the membrane. The DSC transition temperature of the papain fragments is 2−3 deg lower than for the intact protein. However, E was approximately 35 and 45 kcal/mol lower for the unbleached and bleached states, respectively, compared to the intact protein. The chymotrypsin fragment exhibited a drop of 40 kcal/mol in the unbleached state relative to intact rhodopsin. However, in the bleached state two transitions were observed with E of 61 and 48 kcal/mol for the lower and higher melting temperatures, respectively. These peaks are separated by more than 10 °C with the higher transition close to that of opsin.

DISCUSSION

DSC has been used to investigate the thermal stability of rhodopsin in native disk membranes (*13*−*15*) and in disk membranes with altered lipid compositions (*16*, *24*). These studies showed that both the chromophore and the lipid bilayer affect the transition temperature of rhodopsin denaturation. Only one of these earlier studies (*25*) addressed the scan rate dependence of the T_m. The thermal denaturation of rhodopsin is likely to involve multiple steps including isomerization of 11-*cis*-retinal, unfolding of regions exposed to the aqueous media, and/or reorientation of the helices. Because opsin does not have 11-*cis*-retinal, its denaturation would involve the latter two.

The scan rate dependence of the calorimetric transition indicates that during the transition there is significant formation of the final, irreversibly denatured species. This denaturation process is therefore kinetically controlled. The asymmetry of the transition is also consistent with this model. The total enthalpy of the calorimetric transition is nearly identical to E determined from the scan rate dependence of

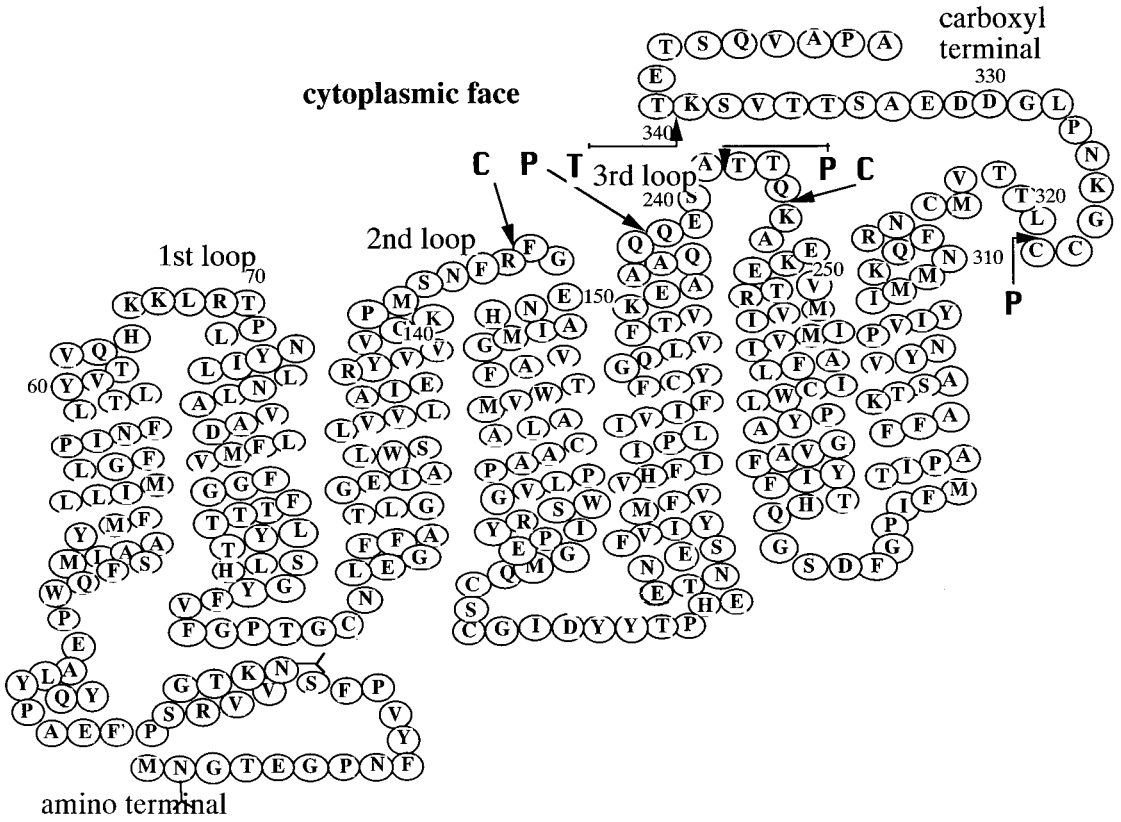

FIGURE 3: Diagram of rhodopsin primary structure [after Hargrave (*40*)] showing sites of proteolysis: T for trypsin; P for papain; C for chymotrypsin.

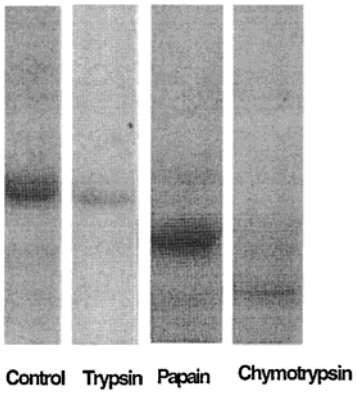

FIGURE 4: Disk membranes were proteolyzed as described in Experimental Procedures. Representative 12.5% SDS−PAGE gels of control disks and disks subjected to proteolysis by trypsin, papain, and chymotrypsin.

Table 2: Transition Temperatures (°C) for Thermal Denaturation of Rhodopsin, Opsin, and the Proteolytic Fragments

	DSC scan rate (deg/min)			
	0.25	0.5	1	1.5
rhodopsin	70.6	71.6	72.5	73.1
opsin	54.3	55.4	56.8	57.5
trypsin				
unbleached	69.5	70.5	71.1	72.2
bleached	52.6	54.0	55.8	56.3
papain				
unbleached	66.8	68.1	68.9	70.2
bleached	45.6	49.4	51.2	52.3
chymotrypsin				
unbleached	65.1	66.4	67.8	68.4
bleached (1)	39.3	42.7	43	44.2
bleached (2)	51	52.2	56.4	57.5

the calorimetric transition temperature. It has been suggested that this may indicate that the transition state consists of a single molecule (rhodopsin or opsin) in a "situation similar to that of the final state" (*19*). The formation of the irreversible state is rapid in comparison to any reversible processes.

The reduction in activation energy upon bleaching suggests that the 11-*cis*-retinal provides a portion of the energy barrier between the native and denatured states. Ligand binding does not always increase the kinetic stability of membrane proteins. While 11-*cis*-retinal increases both the kinetic stabilization and T_m of rhodopsin relative to opsin, the binding of glucose to the GLUT 1 raises the T_m but does not increase the activation energy of thermal denaturation (*26*).

These data on rhodopsin are similar to other studies on membrane proteins. Cytochrome *c* oxidase (*21*), bacteriorhodopsin (*19*), and the GLUT 1 receptor (*26*) have also been shown to undergo thermal denaturation in a kinetically controlled manner. It has been suggested that kinetic constraints may be important factors in the stability of some membrane proteins (*19*, *21*). Although, as described above, multiple states must be present during the transition, the formation of the irreversible final state is rapid with respect to the intermediate states. This can be approximated by a two-state irreversible model.

Several studies have indicated that proteolyzed rhodopsin retains the conformation of the intact protein. Proteolytic fragments of rhodopsin retain their native absorption spectra and the ability to regenerate after bleaching (*22*). Thus the chromophore binding site which involves the helices remains intact after proteolysis. Papain proteolysis does not alter the

helical content of rhodopsin (*23*). Additional studies suggest stabilizing interactions among the intramembranous helices. Proteolytic fragments have been shown to remain associated as a complex after solubilization (*23*, *27*), and some of the helical peptides of both rhodopsin (*28*) (*29*) and bacteriorhodopsin (*30*) spontaneously self-associate in the membrane.

While helix−helix interactions are clearly important, the loops and the carboxyl terminus may also play a role in maintaining overall structural stability. In the case of bacteriorhodopsin it was shown that individual loops accounted for a small stabilizing effect. However, it was projected that in the absence of all loops the bacteriorhodopsin would not be stable at room temperature (*4*).

The role of the cytoplasmic loops and the carboxyl terminus in stabilizing the disk membrane protein, rhodopsin, against thermally induced denaturation was investigated by comparing the behavior of the intact protein to the proteolytic fragments produced upon cleavage of the carboxyl terminus and the cytoplasmic loops. Proteolysis by trypsin has a relatively small effect on the stability of the protein. While the transition temperature is lowered by approximately 1 deg at each scan rate, the activation energy of denaturation as determined by the scan rate dependence of the T_m is essentially unaffected. Upon bleaching, the stabilizing influence of 11-*cis*-retinal is lost. Just as the unbleached trypsin fragment exhibited a stability little changed from the intact rhodopsin, the bleached trypsin fragment differs very little from the intact opsin. This is not surprising since trypsin only removes nine residues from the carboxyl terminus. In the crystal structure this region is not well-defined due to the high *B* values (*9*). However, NMR (*31*, *32*) and FTIR data (*33*) indicate that these residues are involved in the formation of a short stretch of β-sheet. The energy required to break these hydrogen bonds and re-form the hydrogen bonds with water is not large. Therefore, this fragment may dissociate. While it is also possible that the hydrogen bonds are not broken upon proteolysis with trypsin, and the fragment remains associated with the remainder of the protein, this is less likely due to the high solubility of the nine amino acid residue fragment.

The role of the cytoplasmic loops can be investigated using papain and chymotrypsin cleavage. Papain proteolysis cleaves a substantial region of the carboxyl terminus (27 residues) as well as the third cytoplasmic loop. While chymotrypsin does not cleave the carboxyl-terminal residues, both cytoplasmic loops 2 and 3 are cleaved. Upon cleavage by these enzymes, rhodopsin becomes a complex of two (papain) or three (chymotrypsin) helical bundle fragments that maintain the native absorption spectra.

Two aspects of the DSC data should be particularly noted: the number of calorimetric transitions and the activation energy of the denaturation. Prior to bleaching, the fragments produced by papain or by chymotrypsin proteolytic cleavages remain associated strongly enough to exhibit a single calorimetric transition. The denaturation activation energy for both papain and chymotrypsin fragments of rhodopsin is approximately 120 kcal/mol while that for rhodopsin and trypsin fragments is approximately 160 kcal/mol. This suggests that the barrier to denaturation is lowered relative to rhodopsin even while core structural integrity is maintained. The common domain cleaved by both papain and chymotrypsin is the third cytoplasmic loop. It may be coincidental that cleavage of cytoplasmic loop 3 and the carboxyl terminus by papain and cleavage of cytoplasmic loops 2 and 3 by chymotrypsin yield fragments of similar stability. However, it may also suggest that loss of the integrity of the third loop is particularly important in lowering the denaturation activation energy.

In the latter view, the third loop stabilizes the native state relative to the denatured state, suggesting that the transition to the denatured state involves, at least in part, a conformational change in the third loop. Although the crystal structure (*9*) of rhodopsin does not show the third cytoplasmic loop, a new structure (manuscript submitted) derived from nuclear magnetic resonance experiments does show this loop for rhodopsin, as does a recent AFM study (*34*). These studies, as well as recent solution NMR studies on the third cytoplasmic loops from other proteins (*35*, *36*), show an extended helix−turn−helix motif that extends over a significant portion of the cytoplasmic face of rhodopsin (the two other cytoplasmic loops are short in contrast). Therefore, the third cytoplasmic loop may offer a unique stabilization to the protein because of its interactions with other portions of the protein, in particular, the carboxyl terminus and the second cytoplasmic loop.

In the unbleached state, papain-proteolyzed rhodopsin and chymotrypsin-proteolyzed rhodopsin exhibited similar calorimetric behavior. This was not the case after exposure to light. After the papain-proteolyzed disks were bleached, the T_m shifted to a lower temperature and the denaturation activation energy decreased relative to the unbleached state. However, the two fragments consisting of a five-helical bundle and a two-helical bundle produced by papain proteolysis remain associated and exhibited a single calorimetric transition. This suggests favorable interactions at the interface between these fragments even in the absence of retinal. Interestingly, these two fragments will readily dissociate upon bleaching when solubilized in cetyltrimethyl bromide (*23*). Because they apparently remain associated in the bilayer, a role for the lipids in stabilizing the helix interactions is possible.

In contrast to the single transition observed for the bleached papain fragments, the bleached chymotrypsin fragments exhibit two distinct calorimetric transitions. This suggests that the fragments, one three-helical bundle and two two-helical bundles denature as two subunits. Two of the fragments may be interacting strongly with each other and behave as a single unit while the other is independent. It is also possible that the three fragments denature separately, but the two-helical bundles have the same denaturation characteristics and the transitions are indistinguishable. Interestingly, the denaturation activation energy is similar for each of the fragments. In either case, the second cytoplasmic loop must have an important structural role especially in the bleached state.

In the crystal structure (*9*) loop 2 is not well-defined. However, high-resolution NMR determinations of the loop regions indicate that the second cytoplasmic loop is an ordered structure (*37*, *38*). The second cytoplasmic loop is likely important in maintaining the relationship between helix 3 and helix 4 in the bundle of helices and, thus, their interactions with other helices of the bundle. Helix 3 has been shown in the crystal structure to lie largely within the bundle, exhibiting extensive contact with helices 2, 4, 5, and

6 (more helix−helix contacts than any other one helix). This helix is thus central to the helical bundle and its stability, and these data suggest that the second cytoplasmic loop apparently helps to maintain the orientation necessary for these interactions. In this view, the loss of that orientation when loop 2 is proteolyzed reduces the helix−helix interactions sufficiently to enable two sets of helices to denature independently.

These data can be placed in the context of the classes of rhodopsin mutations that lead to retinal degeneration (*39*). Class I mutations are clustered at the carboxyl terminus while class II mutations are in the transmembrane helices and intradiskal loops. Class I mutants exhibit retinal binding, transducin activation, and phosphorylation. Class II mutants show defects in ability to form pigment by binding 11-*cis*-retinal and have been suggested to be less stable than wild-type rhodopsin. Our data demonstrate that the carboxyl-terminal residues play only a small role in rhodopsin or opsin thermal denaturation while the loop regions do play a detectable role. It is possible that class II mutations destabilize the protein so that it denatures more readily in the bilayer, eventually resulting in photoreceptor cell degeneration.

ACKNOWLEDGMENT

We thank Dr. Philip Yeagle for helpful discussions and critical reading of the manuscript. We also thank Drs. Richard Epand, Clare Whiteway, and Anthony Watts for preliminary DSC measurements.

REFERENCES

1. Haltia, T., and Freire, E. (1995) Forces and factors that contribute to the structural stability of membrane proteins, *Biochim. Biophys. Acta 1228*, 1−27.
2. White, S. H., and Wimley, W. C. (1999) Membrane protein folding and stability: physical principles, *Annu. Rev. Biophys. Biomol. Struct. 28*, 319−365.
3. Tajima, S., Enomoto, K., and Sato, R. (1976) Denaturation of cytochrome b5 by guanidine hydrochloride: evidence for independent folding of the hydrophobic and hydrophilic moieties of the cytochrome molecule, *Arch. Biochem. Biophys. 172*, 90−97.
4. Kahn, T. W., Sturtevant, J. M., and Engelman, D. M. (1992) Thermodynamic measurements of contributions of helix-connecting loops and of retinal to the stability of rhodopsin, *Biochemistry 31*, 8829−8839.
5. Marti, T. (1998) Refolding of bacteriorhodopsin from expressed polypeptide fragments, *J. Biol. Chem. 273*, 9312−9322.
6. Papermaster, D., and Dreyer, W. (1974) Rhodopsin content in the outer segment membranes of bovine and frog retinal rods, *Biochemistry 13*, 2438−2444.
7. Smith, H. G., Stubbs, G. W., and Litman, B. J. (1975) The isolation and purification of osmotically intact discs from retinal rod outer segments, *Exp. Eye Res. 20*, 211−217.
8. Unger, V. M., Hargrave, P. A., Baldwin, J. M., and Schertler, G. F. X. (1997) Arrangement of rhodopsin transmembrane α-helices, *Nature 389*, 203−206.
9. Palczewski, K., Kumasaka, T., Hori, T., Behnke, C. A., Motoshima, H., Fox, B. A., Le Trong, I., Teller, D. C., Okada, T., Stenkamp, R. E., Yamamoto, M., and Miyano, M. (2000) Crystal structure of rhodopsin: A G protein-coupled receptor, *Science 289*, 739−745.
10. Ovchinnikov, Y. A. (1982) Rhodopsin and bacteriorhodopsin: structure−functional relationships, *FEBS Lett. 148*, 179−191.
11. Laemmli, U. K. (1970) *Nature 227*, 680−685.
12. Lowry, O. H., Rosenborough, N. J., Farr, A. L., and Randall, R. J. (1951) Protein measurement with the folin phenol reagent, *J. Biol. Chem. 193*, 265−272.
13. Khan, S. M. A., Bolen, W., Hargrave, P. A., Santoro, M. M., and McDowell, J. H. (1991) Differential scanning calorimetry of bovine rhodopsin in rod-outer-segment disk membranes, *Eur. J. Biochem. 200*, 53−59.
14. Miljanich, G. P., Brown, M. F., Mabrey-Gaud, S., and Dratz, E. A. (1985) Thermotropic behavior of retinal rod membranes and dispersions of extracted phospholipids, *J. Membr. Biol. 85*, 79−86.
15. Shnyrov, V. L., and Berman, A. L. (1988) Calorimetric study of thermal denaturation of vertebrate visual pigments, *Biomed. Biochim. Acta 47*, 355−362.
16. Albert, A. D., Boesze-Battaglia, K., Paw, Z., Watts, A., and Epand, R. M. (1996) Effect of cholesterol on rhodopsin stability in disk membranes, *Biochim. Biophys. Acta 1297*, 77−82.
17. Lumry, R., and Eyring, H. (1954) Conformation changes of proteins, *J. Phys. Chem. 58*, 110−120.
18. Freire, E., Osdol, W. W. v., Mayorga, O. L., and Sanchez-Ruiz, J. M. (1990) Calorimetrically determined dynamics of complex unfolding transitions on proteins, *Annu. Rev. Biophys. Chem. 19*, 159−188.
19. Galisteo, M. L., and Sanchez-Ruiz, J. M. (1993) Kinetic study into the irreversible thermal denaturation of bacteriorhodopsin, *Eur. Biophys. J. 22*, 25−30.
20. Sanchez-Ruiz, J. M., Lopez-Lacomba, J. L., Cortijo, M., and Mateo, P. L. (1988) Differential scanning calorimetery of the irreversible thermal denaturation of thermolysin, *Biochemistry 27*, 1648−1652.
21. Morin, P. E., Diggs, D., and Freire, E. (1990) Thermal Stability of Membrane-Reconstituted Yeast Cytochrome *c* Oxidase, *Biochemisty 29*, 781−788.
22. Trayburn, P., Mandel, P., and Virmaux, N. (1974a) Removal of a large fragment of rhodopsin without changes in its spectral properties, by proteolysis of retinal rod outer segments, *FEBS Lett. 38*, 351−353.
23. Albert, A. D., and Litman, B. J. (1978) Independent structural domains in the membrane protein bovine rhodopsin, *Biochemistry 17*, 3893−3900.
24. Polozova, A., and Litman, B. J. (2000) Cholesterol dependent recruitment of di22:6-PC by a G protein-coupled receptor into lateral domains, *Biophys. J. 79*, 2632−2643.
25. Kahn, S. M. A. (1990) Department of Chemistry and Biochemistry *94*.
26. Epand, R. F., Epand, R. M., and Jung, C. Y. (1999) Glucose-induced thremal stabilization of the native conformation of GLUT 1, *Biochemistry 38*, 454−458.
27. Pober, J. S., and Stryer, L. (1975) Letter to the editor: Light dissociates enzymatically cleaved rhodopsin into two different fragments, *J. Mol. Biol. 95*, 477.
28. Ridge, K. D., Lee, S. S. J., and Yao, L. L. (1995) In vivo assembly of rhodopsin from expressed polypeptide fragments, *Proc. Natl. Acad. Sci. U.S.A. 92*, 3204−3208.
29. Yu, H., Kono, M., McKee, T. D., and Oprian, D. D. (1995) A general method for mapping tertiary contacts between amino acid residues in membrane-embedded proteins, *Biochemistry 34*, 14963−14969.
30. Kahn, T. W., and Engelman, D. M. (1992) Bacteriorhodopsin can be refolded from two independently stable transmembrane helices and the complementary five-helix fragment, *Biochemstry 31*, 6144−6151.
31. Yeagle, P. L., Alderfer, J. L., and Albert, A. D. (1995) Structure of the third cytoplasmic loop of bovine rhodopsin, *Biochemistry 34*, 14621−14625.
32. Yeagle, P. L., Alderfer, J. L., and Albert, A. D. (1996) Structure determination of the fourth cytoplasmic loop and carboxyl terminal domain of bovine rhodopsin, *Mol. Vision 2*, http://www.molvis.org/molvis/v2/p12/.
33. Pistorius, A. M., and deGrip, W. J. (1994) Rhodopsin's secondary structure revisited: assignment of structural elements, *Biochem. Biophys. Res. Commun. 198*, 1040−1045.

34. Jeymann, J. B., Pfeiffer, M., Hildebrandt, V., Kaback, H. R., Fotiadis, D., Groot, B. d., Engel, A., Oestserhelt, D., and Miller, D. J. (2000) Conformations of the rhodopsin third cytoplasmic loop grafted onto bacteriorhodopsin, *Structure 8*, 643−653.
35. Mierke, D. F., Royo, M., Pelligrini, M., Sun, H., and Chorev, M. (1996) Third cytoplasmic loop of the PTH/PTHrP receptor, *J. Am. Chem. Soc. 118*, 8998−9004.
36. Franzoni, L., Nicastro, G., Pertinhez, T. A., Oliveira, E., Nakaie, C. R., Paiva, A. C., Schreier, S., and Spisni, A. (1999) Structure of two fragments of the third cytoplasmic loop of the rat angiotensin II AT1A receptor. Implications with respect to receptor activation and G-protein selection and coupling, *J. Biol. Chem. 274*, 227−235.
37. Yeagle, P. L., Alderfer, J. L., and Albert, A. D. (1997) The first and second cytoplasmic loops of the G-protein receptor, rhodopsin, independently form β-turns, *Biochemistry 36*, 3864−3869.
38. Yeagle, P. L., Alderfer, J. L., and Albert, A. D. (1997) Three-dimensional structure of the cytoplasmic face of the G protein receptor rhodopsin, *Biochemistry 36*, 9649−9654.
39. Sung, C. H., Davenport, C. M., and Nathans, J. (1993) Rhodopsin mutations responsible for autosomal dominant retinitis pigmentosa, *J. Biol. Chem. 268*, 26645−26649.
40. Hargrave, P. A., McDowell, J. H., Curtis, D. R., Wang, J. K., Juszczak, E., Fong, S. L., Rao, J. K. M., and Argos, P. (1983) The structure of bovine rhodopsin, *Biophys. Struct. Mech. 9*, 235−244.

BI0100539